



Publication Year	2024
Acceptance in OA	2025-04-02T10:06:42Z
Title	Machine learning applied to fiber-fed focal plane wavefront sensing: a study of aberrated wave transmission through multimode optical fibers
Authors	DI FRANCESCO, Benedetta, DI FRISCHIA, Stefano, DI RICO, Gianluca, DOLCI, Mauro, DI ANTONIO, Ivan, Harris, Robert J., TOZZI, Andrea, IUZZOLINO, Marcella
Publisher's version (DOI)	10.1117/12.3017944
Handle	http://hdl.handle.net/20.500.12386/37001
Serie	PROCEEDINGS OF SPIE
Volume	13100

Machine Learning applied to fiber-fed focal plane wavefront sensors: a study of aberrated wave transmission through multimode optical fibers

Benedetta Di Francesco ^{a,b}, Stefano Di Frischia^a, Gianluca Di Rico^a, Mauro Dolci^a, Ivan Di Antonio^a, Robert J. Harris^c, Andrea Tozzi^d, and Marcella Iuzzolino^d

^aINAF, Osservatorio Astronomico d'Abruzzo, Via Mentore Maggini, snc, Teramo, Italy

^bDipartimento di Fisica, Università di Roma Tor Vergata, Via della Ricerca Scientifica, 1, Roma, Italy

^cCentre for Advanced Instrumentation, Department of Physics, Durham University, United Kingdom

^dINAF, Osservatorio Astrofisico di Arcetri, Largo Enrico Fermi, 5, Firenze, Italy

ABSTRACT

This research explores the potential of machine learning and neural networks in recognizing the input features of aberrated wavefronts transmitted through multimode optical fibers, in view of applications for wavefront sensing in ground-based telescopes. Recent studies highlight the efficacy of multimode fibers for imaging and sensing, suggesting neural networks' effectiveness in mapping relationships between output distortions and input wavefront aberrations. The initial step of our study concerned multimode fiber propagation simulations. An input Gaussian beam was distorted with known aberrations and then sent through the fiber to analyze the effects on the output. This groundwork was used to train and validate a Convolutional Neural Network architecture. Its main role was to understand, from output images, which type of aberration was superimposed in input. We obtained promising results with test accuracy of 85% and 87%, while achieving good performance in network training and generalization.

Keywords: optical fibers, wavefront sensing, adaptive optics, machine learning, neural networks, astrophotonics

1. OPTICAL FIBERS IN SENSING APPLICATIONS

Optical fibers are photonic waveguides able to transmit light over a given distance. In telecommunications, they play a fundamental role for data transmission and internet connectivity. Due to their compactness, easy availability, and flexibility, these devices can adapt to various fields. In the industrial sector, they are widely used as sensors for micro-vibration, temperature, and pressure variations. In the medical field, they are employed as probes in endoscopy, ophthalmology, and bio-imaging.

Until the last decade, their usage in astronomy was confined to certain instruments, primarily spectrographs for Integral Field Spectroscopy (IFS) and Multi-Object Spectroscopy (MOS). With the emergence of optical fiber imaging and sensing, new possibilities have arisen, notably in the field of Adaptive Optics (AO) where wavefront sensing poses a significant challenge. Despite the existence of several wavefront sensors (Shack-Hartmann, pyramid, curvature sensors...), new fiber-fed Focal Plane Wavefront Sensors (FP-WFS) are emerging. Recent studies^{1,2} have examined the effectiveness of devices known as Photonic Lanterns (PLs) in measuring aberrations at the telescope focal plane.

Our research explores the potential use of Multimode Fiber (MMF) for wavefront sensing.

This concept is non-trivial, especially considering that MMFs are highly scattering media. They are capable of supporting multiple transmission modes with different propagation constants. The light launched into the fiber

Further author information:

E-mail: benedetta.difrancesco@inaf.it , Telephone: +39 0861 439 739

undergoes mode-mixing, resulting in a random intensity distribution known as "speckle." From this pattern, determining the input to the fiber is not straightforward. Various mathematical models have been proposed to understand the input/output relationship, including analog phase conjugation, digital iterative methods, or transmission matrix recovery. However, these methods are computationally intensive and not suitable for real-time applications. In this complex context, Machine Learning (ML) based approaches are good candidates to avoid heavy computation and gain fast reconstruction.

In recent studies, the possibility to imaging and sensing through multimode fiber with the aid of well-trained neural network have shown important promises.

In detail, B. Rahmani et al.³ used multimode fiber to transmit letters from Latin alphabet verifying the output reconstruction accuracy with machine learning. The letters were first imaged onto a Spatial Light Modulator (SLM) and then transmitted through a multimode fiber. The resulting speckles were recorded and used to train a neural network. High accuracy was achieved in determining the sent letter, despite the initial information being scattered by the combination of modes.

In an analogue way, D. Zheng et al.⁴ examined the effect of atmospheric turbulence on a light beam injected into a Few Mode Fiber (FMF). Also in this case, the beam was distorted by a phase modulator (SLM) reproducing the effect of atmospheric aberration and the resulting intensity distribution at the output was examined. This process allowed for the sensing of atmospheric effects on the fiber's output.

Unlike the previous scenario, where the turbulence on the input beam was given by an atmospheric law, the aberrations in our study are defined by known Zernike polynomials, which add as a phase terms to an initial Gaussian field.

After introducing this phase distortion, we simulated the transmission through an MMF with known physical properties, collecting intensity images at the output facet. With the aid of a Convolutional Neural Network (CNN), we studied the accuracy of machine learning-based methods in recognizing the input aberration.

Our findings shed light on the feasibility of using CNN for aberration sensing, underscoring the synergy between neural network and photonics.

2. METHODS

The study could be divided in two parts. The first is related to the propagation simulation through a MMF, done with a specific software in MATLAB. This step reveals fundamental to collect proper training images for the neural network. The second part focuses on the architecture of the CNN with training, validation and test steps.

2.1 Propagation simulations and images acquisition

The simulations were done using the Beam Propagation Method (BPM) software⁵ in MATLAB, which is able to reproduce optical propagation through waveguides with given geometrical and physical properties.

The fiber, used to transmit a monochromatic light of $\lambda = 800 \text{ nm}$, has a core of $50 \mu\text{m}$ and a length $L = 10 \text{ cm}$. This length was chosen as a trade off between time consumption and number of simulations. In fact, to acquire as many output images as possible, the length must be controlled.

The core and cladding refractive indexes of the fiber were determined in such a way that the numerical aperture NA was equal to 0.20.

In case of normal conditions, where there is no distortion in the light launched into the MMF, the initial input field U_i can be considered as a bi-dimensional Gaussian distribution function:

$$U_i = A \exp\left(-\frac{x^2 + y^2}{w^2}\right), \quad (1)$$

where:

- A is the amplitude. For simplicity, it was put equal to 1
- w is proportional to half of the fiber core diameter

Equation (1) represents the field at the input facet of the fiber, with no additive phase term. To create a given distortion, we added aberrations in the form of Zernike polynomial to the phase of U_i . Zernike polynomials are a set of orthogonal polynomials defined on an unit disk, which are widely used in optics and wavefront analysis. They efficiently decompose wavefronts into a series of polynomials characterized by a radial degree n and an azimuthal degree m . Therefore each polynomial represents a specific phase distortion on a wavefront. In this work, six different Zernike terms were considered: Tip, Tilt, Defocus and the combinations of these three (Tip + Tilt, Tip + Defocus and Tilt + Defocus).

Table 1: n and m values of the aberrations used

Aberration	n	m
Tip (horizontal, X-tilt)	1	1
Tilt (vertical, Y-tilt)	1	-1
Defocus	2	0

For each aberration, the Zernike polynomial is in the form:⁶

$$Z_{n,m}(r, \theta) = \begin{cases} R_{n,m}(r) \cos(m\theta) & \text{for } m \geq 0 \\ R_{n,m}(r) \sin(m\theta) & \text{for } m < 0 \end{cases}$$

where $0 \leq r \leq 1$ is the radius of unit circle, θ is the corresponding angle and $R_{n,m}(r)$ is defined as:

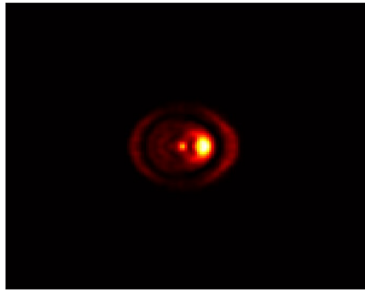
$$R_{n,m}(r) = \sum_{l=0}^{\frac{n-m}{2}} = \frac{-1^l (n-l)!}{l! [\frac{1}{2}(n+m) - l]! [\frac{1}{2}(n-m) - l]!} r^{n-2l} \quad (2)$$

From this point, we will refer to the Zernike polynomials just as $Z_{n,m}$ for better readability. Therefore, after applying the previous equation to compute them, they were added as a phase term to U_i :

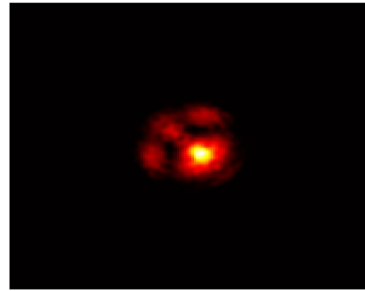
$$U = U_i \exp(-j\pi b Z_{n,m}), \quad (3)$$

where b defines the intensity of the aberration.

Once the input field was distorted, it was sent through the fiber, giving as output a new field distribution U_o . Its intensity $|U_o|^2$ was saved as image together with the label corresponding to the superimposed $Z_{n,m}$ term. Some examples are reported in the Figure 1.



((a)) Tip + Defocus with $b = 0.2$



((b)) Tip + Tilt with $b = 0.1$

Figure 1: Fiber output intensity

Along with applying Zernike polynomials to the initial phase of the input Gaussian field, we also tested the fiber

output under bending conditions, adding to the fiber a given Radius of Curvature (RoC). It is defined as the radius of the circle that closely matches the bend in the fiber at a specific point, quantifying the sharpness of the bend.

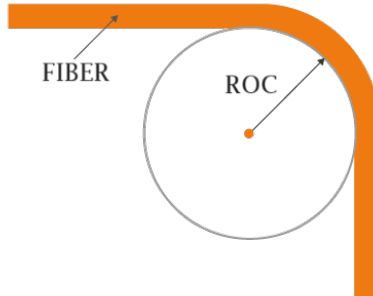


Figure 2: RoC in a bent fiber

In practical scenarios, optical fibers transmit signals inside the core region via Total Internal Reflection (TIR). For this process to occur, the light must enter in the fiber and being continuously reflected between the core and the cladding at angles greater than a critical threshold. Bending losses happen when light traveling through the fiber escapes the core, either entering the cladding or leaving the fiber entirely, leading to a signal power loss. In real situation it could happen that the fiber is not always straight, due to movements of the instrumentations or due to the path it has to follow. Therefore we decided to analyze this factor. When the fiber is bent, there is a local change in the refractive index.⁷ This different behaviour of refractive index could influence the output beyond the input Zernike aberrations applied. In Figure 3, it is evident that, despite the presence of the same input aberrations displayed in Figure 1, the output shows certain unseen characteristics with reduced light power.



((a)) Tip + Defocus with RoC

((b)) Tip + Tilt with given RoC

Figure 3: Fiber output intensity with given RoC

In both cases, with or without bending, we created a correspondence between an input phase aberration and an output intensity image. These elements were used to train and test the CNN in recognizing the aberration from the image provided.

2.2 CNN architecture with training and validation sets

The CNN was built in Python, using TensorFlow and Keras. It receives as input a 160x160x3 image. The structure is depicted in Figure 4 and the layers are here listed:

- First Convolutional Layer with 32 filters and ReLu activation function
- First Max Pooling (2x2)
- Second Convolutional Layer with 64 filters and ReLu activation function
- Second Max Pooling (2x2)
- Third Convolutional Layer with 128 filters and ReLu activation function
- Third Max Pooling (2x2)
- Flatten Layer
- Dense Layer
- Fully Connected Layer
- Output with 6 labels corresponding to the superimposed Zernike terms

It is worth mentioning also that each convolutional layer has a Kernel size of 3x3, the classification in the last layer is done through SoftMax activation function and that the model compiler uses an Adam optimizer with a learning rate of 0.001.

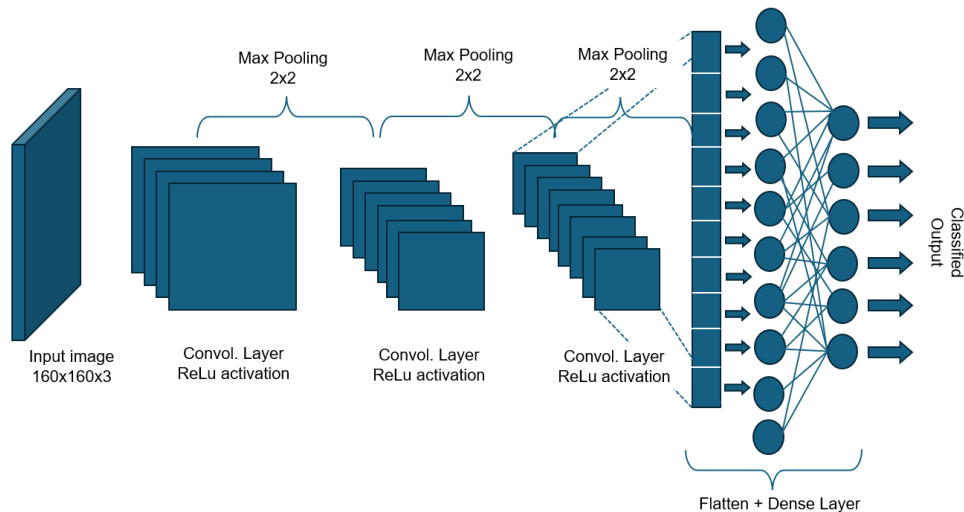


Figure 4: CNN structure layers and architecture

Every CNN requires high number of data to be trained, validated and tested.

For the training set we used images from the simulations that could recreate real operating conditions. In particular, we moved b from 0.1 to 0.5 for each aberrations and we also added specific *RoCs*, moving it from $5 \times 10^{-2} m$ to $10^{-1} m$. On our first attempt, we collected 6000 images.

In this way we registered the behaviour of the fiber when it was bent or when the incoming phase aberration increased.

Before running the neural network, the training set was split to create validation set, used in the model fitting. The split ratios between training set and validation set were chosen to be 80% - 20%. Moreover, to overcome the simulation duration while having enough training images, we decided to perform Data Augmentation in TensorFlow. Starting from the simulated images, the new augmented outcomes were zoomed, rotated and flipped images. This guaranteed better training consistency. Once both simulated and augmented data were collected, the model fitting started. During this step, the batch size was set to 32 and it was provided an early stopping system to halt training when validation performance did not improve.

With 50 epochs, the neural network performed a good learning process. The four main parameters to keep under control were: training and validation accuracies on one side and training and validation losses on the other side. The training accuracy is the percentage of correct predictions the model makes on the training dataset. It measures how well the model has learned the patterns in the data it was trained on. The training loss, instead, quantifies the error between the predicted outputs and the actual outputs in the training dataset. In similar way, the validation accuracy is the percentage of correct predictions the model makes on the validation dataset and it measures how well the model generalizes to new, unseen data. The validation loss quantifies the error between the predicted outputs and the actual outputs in the validation dataset. It is worth mentioning that the two accuracy values must grow together, without significant gap one from the other. The same stands for the two loss values. A large gap in both cases can indicate overfitting or bad network generalization. The results are reported below.

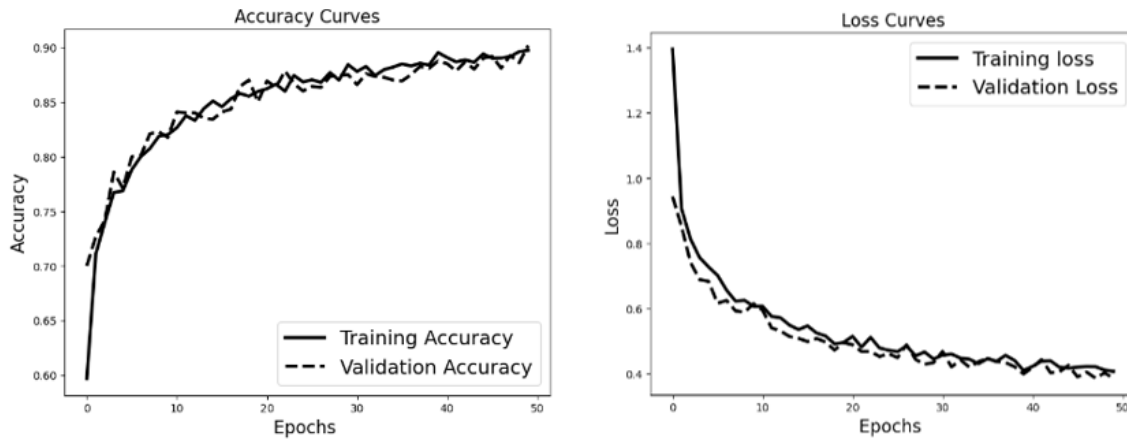


Figure 5: CNN accuracy and loss values during training step

Based on the plots, it is evident that:

- accuracy is increasing: both training and validation accuracy improve consistently during epochs, reaching high values (90 % for training and 89% for validation)
- there is an evident loss reduction: it indicates effective learning
- neural network shows small accuracy gap: model is generalizing without significant overfitting

3. RESULTS AND DISCUSSION

The performance was evaluated giving to the model three test sets, each composed of 1000 images, containing also unseen data. The test sets were created changing the parameter of interests, b and RoC .

Table 2: Test sets

Number of test set	b	$RoC [m]$
#1	[0.1, 0.9]	∞
#2	0.2	$[10^{-2}, 10^{-1}]$
#3	[0.1, 0.9]	$[10^{-2}, 5 \times 10^{-2}]$

In the first test set, we concentrated more on the b parameter, therefore, this test wanted to check how the network performed in case the aberration contributions increased. Moving it randomly in the range $b \in [0.1, 0.9]$, we explored the model evaluation with unseen data. In fact, the network was trained only with $b \in [0.1, 0.5]$. In the Figure 6 we show the confusion matrix. The total test accuracy achieved was 85%. The result explains that, in the absence of bending, the network is capable of detecting the input phase aberration, even when it is significant. This is a promising finding because for a potential use in astronomical instrumentations, it demonstrates how preserving the mechanical stability of the fiber is crucial for optimal sensing.

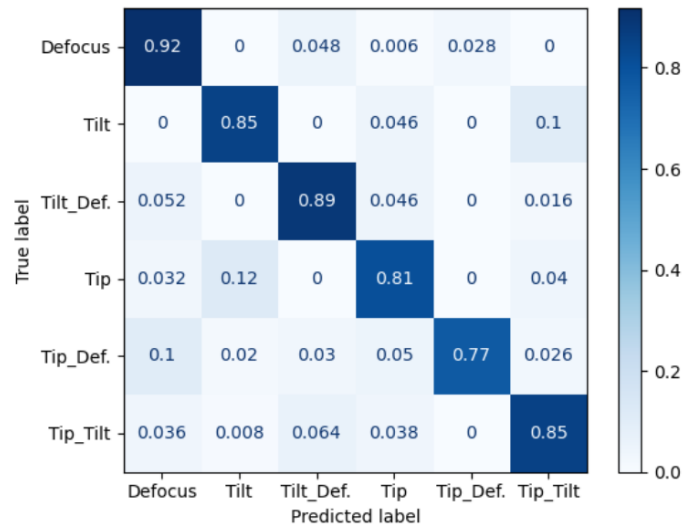


Figure 6: Confusion matrix for the first test set

In the second test set, while keeping fixed the intensity of Zernike aberration, the fiber was bent quite severely, even more than real-life situation. However, the performance obtained with the test accuracy reaches the 87%.

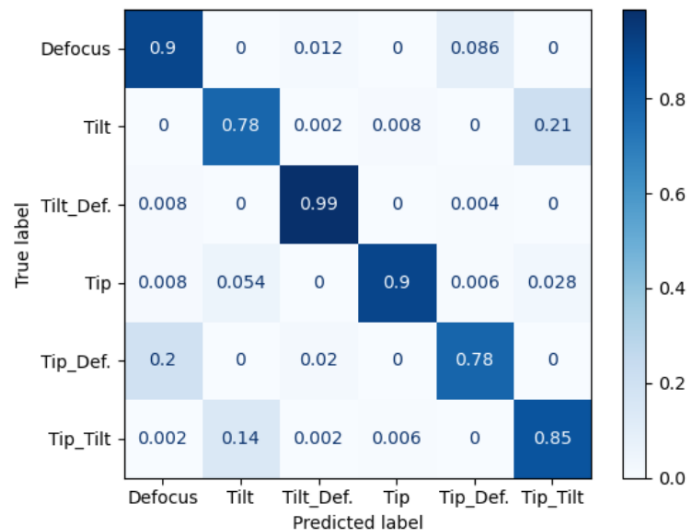


Figure 7: Confusion matrix for the second test set

The first thing to notice is that the test accuracy values are reasonably close to the training and validation ones. A slight drop is expected and acceptable. It indicates that the model is performing well on unseen data, and the

differences could be due to natural variations in the datasets.

Moreover, in the two confusion matrices, it is possible to see that for some aberrations (Defocus, Tip + Defocus and Tip + Tilt) the behaviour of the network is the same. There are slight changes in the Tilt and Tip separately, while observing increasing performance in the Tilt + Defocus case. This may be due to the fact that, even with a significant *RoC*, when the impact of Zernike is not so high, the training data are sufficient to generalize. This also demonstrates that the impact of phase aberrations is more detrimental compared to severe bending of the fiber.

The third test set yielded a very low test accuracy (less than 60%). In this case, it is evident that while it's true that with severe bending and low Zernike impact, the network is still able to track the behavior of fiber output, the same cannot be said for higher Zernike values. Therefore, the latest test confirms the conclusions we found for the other two sets.

Based on the results, we have identified two distinct issues that need addressing:

- network complexity: enhancements could be made by adjusting the number of convolutional layers.
- network training: it is necessary to gather additional images with greater Zernike intensity and retrain the network

4. CONCLUSION AND FUTURE WORK

This work has provided an initial investigation of the problem. In the upcoming period, it will be necessary to generalize the problem further. Initially, we will need to work with many more Zernike modes and standardize the network's complexity to facilitate learning the new aberrations. Additionally, while we have assigned very small values to the *RoC* so far, we realize that in a realistic scenario, fiber stability conditions must be imposed. Alternatively, it would be better to consider how the fiber, and consequently the network, behaves under vibrations. Another issue to address is the polychromatic nature of light, which is more realistic than the monochromatic one for the fields of interest. To overcome this obstacle, the best approach is to test the system on an optical bench in the laboratory and observe the network's response to different wavelengths. In this specific case, a software-controlled phase modulator will inject a known aberration into the fiber while a camera captures images and collects data. The network architecture can be maintained as it is, unless further training is required for proper operations.

In any case, this will enable us to determine if additional characteristics that we have not yet considered could heavily affect the system, such as variations in core diameter or in the light incidence angle at the fiber input. In conclusion, these preliminary results have shown that there is a possibility of finding a method to define the correspondance between the aberrations at the input of MMF and the recorded output intensity. Indeed, the model demonstrates robust performance, with consistent results across training, validation and test sets. While achieving accuracies of $\approx 90\%$ in both training and validation, the slight drop to 85% and 87% in the two separate test sets is within an acceptable range. This suggests the model generalizes well to the data, affirming its reliability and effectiveness, however further training iterations and more complex scenarios are necessary for future development.

REFERENCES

- [1] Corrigan, M., Morris, T., Harris, R., and Anagnos, T., “Demonstration of a photonic lantern low order wavefront sensor using an adaptive optics testbed,” 202 (07 2018).
- [2] Norris, B., Wei, J., Betters, C., Wong, A., and Leon-Saval, S., “An all-photonic focal-plane wavefront sensor,” *Nature Communications* **11** (10 2020).
- [3] Rahmani, B., Loterie, D., Konstantinou, G., Psaltis, D., and Moser, C., “Multimode optical fiber transmission with a deep learning network,” (05 2018).
- [4] Zheng, D., Li, Y., Li, B., Li, W., Chen, E., and Wu, J., “Free space to few-mode fiber coupling efficiency improvement with adaptive optics under atmospheric turbulence,” (03 2017).
- [5] Veettikazhy, M., Hansen, A. K., Marti, D., Jensen, S. M., Borre, A. L., Andresen, E. R., Dholakia, K., and Andersen, P. E., “Bpm-matlab: an open-source optical propagation simulation tool in matlab,” *Opt. Express* **29**, 11819–11832 (Apr 2021).
- [6] Lakshminarayanan, V. and Fleck, A., “Zernike polynomials: A guide,” *Journal of Modern Optics - J MOD OPTIC* **58**, 1678–1678 (04 2011).
- [7] Kiiveri, P., Kuusisto, M., Koponen, J., Kimmelma, O., Aallos, V., Harra, J., Husu, H., and Kyllönen, P., “Refractive index profiles and propagation losses in bent optical fibers,” *Optical Engineering* **61**(12), 126106–126106 (2022).